

Short Communication

Effect of Natrium Hydroxide Concentration on the Properties of ZnO Thin Film Nanotubes and the Performance of Dye-sensitized Solar Cell

M.Y.A. Rahman*, L. Roza, A.A. Umar[#], M.M. Salleh

Institute of Microengineering and Nanoelectronics (IMEN), Universiti Kebangsaan Malaysia, 43600, Bangi, Selangor, Malaysia.

E-mails Addresses: mohd.yusri@ukm.edu.my*; akrajas@ukm.edu.my[#]

Received: 12 January 2015 / Accepted: 23 February 2015 / Published: 4 March 2015

ABSTRACT: The synthesis parameter of thin film photovoltaic materials plays important role on their properties and the performance of DSSC. ZnO thin film nanotubes which serve as a photovoltaic material in DSSC was synthesized via seed mediated hydrothermal technique. The effect of natrium hydroxide (NaOH) precursor concentration at constant hexamethylenetetramine (HMT) surfactant and zinc nitrate $[Zn(NO_3)_2]$ concentration on the morphology, optical absorption and the performance of the dye-sensitized solar cell (DSSC) utilizing the ZnO samples has been investigated. The samples were characterized by field emission scanning electron microscopy (FESEM), energy dispersive X-ray (EDX) and ultraviolet-visible optical absorption techniques. The DSSC was tested under dark condition and under illumination of 100 mW cm^{-2} light from tungsten halogen lamp. It was found that the morphology and optical absorption of ZnO nanostructure are significantly affected by the NaOH concentration. The diameter of the ZnO nanotubes decreases as the precursor concentration increases. The device does not show rectification property in dark. The photovoltaic parameters increase with the decrease in the NaOH concentration. The DSSC utilizing ZnO nanotubes synthesized at 0.005 M NaOH performs the J_{sc} , V_{oc} , FF and η of 0.80 mA cm^{-2} , 0.38 V , 0.388 and 0.103% , respectively. The highest performance of that cell is due to the broadest absorption window of 0.005 M sample.

Keywords: DSSC; Hydrothermal; NaOH; Nanotube

1. Introduction

ZnO is a metal oxide semiconductor which is an alternative photovoltaic material to TiO_2 since it exhibits high electrochemical stability and superior electron mobility [1, 2]. ZnO is being studied extensively as a promising candidate in a photoelectrochemical cell (PEC) and dye-sensitized solar cell (DSSC) since it is cheap and easy to synthesize in film form in a large variety of nanostructure morphologies [3, 4]. In order to utilize the nanostructure material, it usually requires that the crystalline morphology and shape of nanostructures can be controlled during the synthesis processes [5-6]. Several techniques have been employed to produce ZnO nanostructures such as doctor blade technique [7], hydrolysis technique [8, 9] and hydrothermal process [10]. Several properties of photovoltaic material such as morphology, thickness and optical properties obtained by varying the synthesis parameters of photovoltaic materials affected the performance of the PEC and DSSC [11-14].

In this work, we have employed hydrothermal technique to synthesize ZnO nanotube. In this technique, natrium hydroxide (NaOH) precursor was added in a growth solution containing $Zn(NO_3)_2$ and hexamethylenetetramine (HMT). The new idea of the work is that the addition of NaOH into the growth solution was to control the morphological nanostructure of ZnO at nanotube shape. The goal of the work is to investigate the influence of NaOH concentration at fixed HMT and $Zn(NO_3)_2$ concentration on the morphology and optical absorption of the ZnO thin films and the performance of

the DSSC utilizing the ZnO samples.

2. Experimental

The ZnO films were grown on fluorine-tin oxide (FTO) substrate via simple seed mediated hydrothermal technique. This method involved two route steps, namely, seeding process by deposition of zinc acetate dihydrate $[Zn(CH_3COO)_2 \cdot 2H_2O]$ solution on FTO substrate to prepare uniform ZnO nanoseed and followed by the growth process in aqueous solution of zinc nitrate hexahydrate $[Zn(NO_3)_2 \cdot 6H_2O]$ and HMT. Reagent grade $Zn(NO_3)_2 \cdot 6H_2O$ and HMT powders ($\geq 99.0\%$ in purity) were used as precursors without any purification. Before seeding process, the substrates were cleaned using a standard cleaning procedure in acetone, 2-propanol and ethanol for 15 minutes in ultrasonic bath, respectively. The substrates were then dried under nitrogen flow. After the cleaning treatment, the substrates were used immediately for growth process.

2.1 Seeding Process

ZnO nanoseeds on the FTO surface were prepared using an alcohol-thermal seeding method. A thin layer of ethanolic solution of 10 mM zinc acetate dihydrate $[Zn(CH_3COO)_2 \cdot 2H_2O]$ on a cleaned FTO surface was firstly prepared by two-steps spin-coating process for 6 seconds at 400 rpm and followed for 30 seconds at 3000 rpm to make sure the solution was evenly distributed on the substrate and to get the sufficient thickness of the seed growth on the substrate. The sample was then dried at 100

°C on a hot-plate for 15 minutes and then cooled down to 60 °C. These procedures were repeated three times in order to get appropriate thickness of ZnO nanoseeds. The sample was annealed in air at 350 °C for 1 hour inside a horizontal tube furnace.

2.2 Growth Process

The sample was subsequently immersed in a growth solution. The growth of ZnO nanostructures from the nanoseeds was carried out by immersing the nanoseeds-attached FTO in a equimolar solution, 0.040 M of $Zn(NO_3)_2 \cdot 6H_2O$ and HMT. Then, 0.050 M NaOH was added into the solution and the growth reaction was carried out at 90 °C for 8 h inside an electric oven. The substrate with ZnO seed layer was put face down in the growth solution with the angle between the substrate and beaker bottom was 45°. After heating for 8 h at 90 °C, the solution was subsequently cooled down to 50 °C and the reaction was left for 16 h. After the growth process, the samples were then taken out and washed several times using pure water in order to remove any precipitation on their surface and dried using a flow of nitrogen gas for characterizations. These procedures were repeated for the 0.010, 0.015 and 0.030 M NaOH.

The morphology of the ZnO nanostructures was observed using field-emission scanning electron microscopy (FESEM) analysis (Zeiss Supra 55VP FESEM) with the magnification of 50000 X. The diameter of the ZnO nanotubes was estimated using a scale bar located at the lower right corner of the FESEM micrographs and illustrated in **Table 1**. The average diameter was taken from the analysis on ten ZnO nanotubes. Energy dispersive X-ray (EDX) spectrometer was employed for the elemental analysis on the 0.005 M sample. Optical spectrophotometer UV-Vis Lambda 900 Perkin Elmer was employed to study the optical absorption of the ZnO sample. The absorbance of the films was measured in the wavelength ranging from 300 to 900 nm.

2.3 Fabrication and performance study of DSSC

The ZnO nanotubes samples were utilized in dye-sensitized solar cells (DSSC). For the device fabrication, the ZnO samples were immersed into an ethanolic solution of 0.3 mM N719 dye for 2 h. The samples were then taken out, rinsed gently with fresh ethanol and then dried under a flow of nitrogen gas. Platinum film as a counter electrode was prepared by sputtering platinum pellets on the ITO substrate. An electrolyte containing 0.5 M LiI/0.05 M I_2 /0.5 M TBP in acetonitrile was used as a redox couple. A DSSC was fabricated by sandwiching the parafilm between ZnO nanstructure and platinum counter electrode and clamped in order to optimize the interfacial contact between the components making up the cell. The electrolyte was injected into the cell and filled via a capillary. The performance study of the cell was carried out by observing the current-voltage in the dark and under illumination using an AM 1.5 simulated light with an intensity of 100 mW cm^{-2} from tungsten halogen lamp. The intensity of the light was measured using solar simulator. The illuminated circular area of the cell was 0.23 cm^2 . The current-voltage curves in the dark and under illumination were recorded by a Keithley high-voltage source model 237 interfaced with a personal computer.

3. Results and discussion

Figure 1 shows the FESEM micrographs for the ZnO nanotubes grown at various NaOH concentrations. The morphology of the nanotubes is inhomogeneous. It was found that the compact nanostructural shape of the ZnO particle is nanotube observed from the FESEM images. The most dense and compact structure is observed for the 0.010 M sample. The nanotube diameter decreases as the NaOH concentration increases from 0.005 M to 0.030 M as illustrated in **Table 1**. At 0.030 M NaOH, the morphology of the ZnO nanotubes become less compact since the dissolution rate is faster at higher concentration

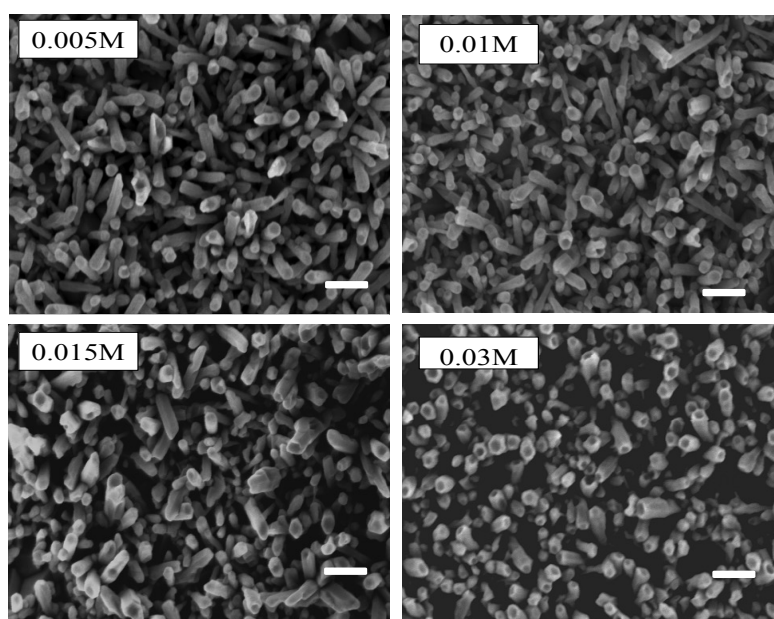


Figure 1: FESEM micrographs of the ZnO nanotubes grown at various NaOH concentrations. Scale bars are 200 nm

Table 1: Diameter of ZnO nanotubes and photovoltaic parameters of the DSSCs utilizing ZnO nanotubes grown at various NaOH concentrations

Concentration (M)	Diameter (nm)	V_{OC} (V)	J_{sc} (mA cm ⁻²)	FF	η (%)
0.005	80±8	0.38	0.80	0.39	0.103
0.010	77±6	0.38	0.75	0.35	0.101
0.015	68±9	0.38	0.67	0.35	0.084
0.030	59±9	0.40	0.46	0.33	0.061

during the growth process. At lower concentration, the particles agglomerate and form colloids, thus causing the nanotubes size to increase.

Figure 2 shows the EDX spectrum of the ZnO sample deposited on the FTO substrate at 0.005 M NaOH. The spectrum is only presented for the 0.005 M sample since the spectra for the other concentration samples show quite similar pattern to that of the 0.005 M sample. The spectrum reveals that the elements forming ZnO nanotubes exist in the sample with Zn element exists at higher atomic percentage than O element.

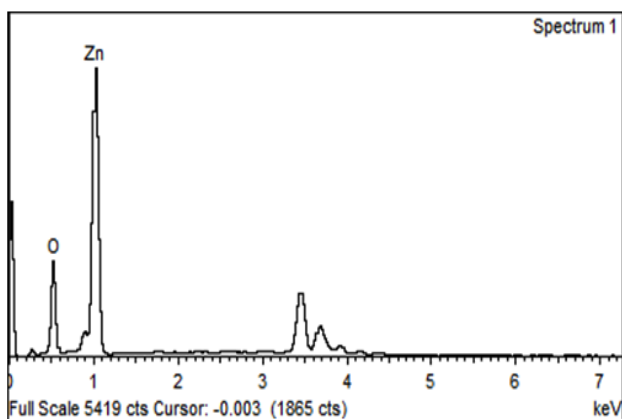
**Figure 2:** EDX spectrum of the ZnO nanotubes grown at 0.005 M NaOH

Figure 3 shows the UV-Vis spectra for the ZnO nanotubes grown on the substrate at various NaOH concentrations. It is found that the samples show high optical absorption in the UV region in the range from 300-380 nm and low absorption in the visible to infrared region ranging from 380-900 nm. The 0.005 M sample possesses the largest absorption window or absorption area followed by the 0.015, 0.010 and 0.030 M samples. This is due to the 0.005 M sample has the largest nanotube diameter and the 0.030 M samples demonstrates the less dense nanotube structure. The sample with the highest diameter absorbs more light and the one with the less compact structure absorbs less light. It also noticed that the 0.010 M sample shows the highest absorption peak at 320 nm followed by 0.005, 0.015 and 0.030 M samples. From the figure, it is seen that the energy gap of the samples does not significantly change with NaOH concentration.

Figure 4 illustrates the I - V curve in dark of the device utilizing the sample deposited on the substrate at 0.005 M NaOH. It is noticed that the dark current in the reverse bias is slightly higher than that in the forward bias. Thus, the

device does not allow the current to be dominant in one direction either in forward or reverse bias. In other words, the device does not act as a rectifier [15, 16]. However, the dark current in the device is significantly high which is in the range of mA. This will result in high photocurrent and power conversion efficiency once the device is illuminated with light.

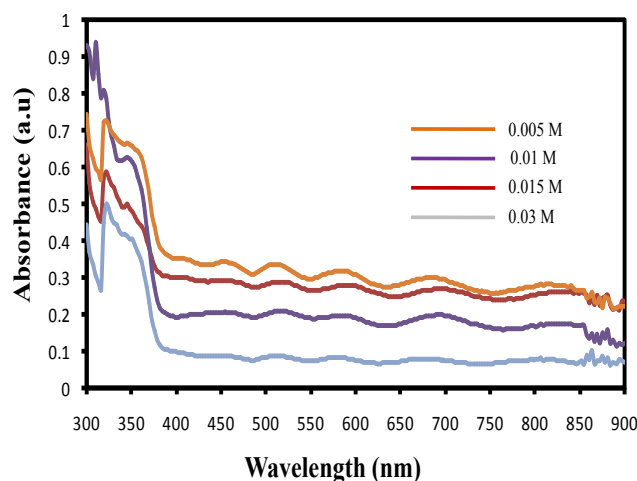
**Figure 3:** UV-Vis spectra for the ZnO nanotubes grown at various NaOH concentrations

Figure 5 shows the J - V curves of the DSSCs utilizing the ZnO samples prepared at various NaOH concentrations. The curves do not follow the shape of that of silicon solar cell, leading to low fill factor (FF) illustrated in **Table 1**. The photovoltaic parameters are analyzed from **Figure 5** and illustrated in **Table 1**. From the table, it is clearly seen that the J_{sc} , V_{oc} and η decrease with NaOH concentration. However, this trend is not seen for V_{oc} . The cell utilizing the ZnO nanotubes grown at 0.005 M NaOH demonstrates the highest J_{sc} and η while that utilizing the sample prepared at 0.030 M NaOH performs the lowest J_{sc} and η . The increase in J_{sc} and η with the concentration could be explained by the UV-Vis results shown in **Figure 3**. The ZnO sample grown at 0.005 M possesses the broadest absorption window. This sample absorbs the highest number of photon and consequently generates the highest number of electron-hole pairs. Thus, the J_{sc} and η are improved. Generally, the highest J_{sc} and η obtained from this work are regarded lower compared with those obtained by the other researchers [17-21]. This might be due to the sensitization effect of the N719 dye loading into ZnO films in this work is smaller than those reported in [17-21]. The smaller

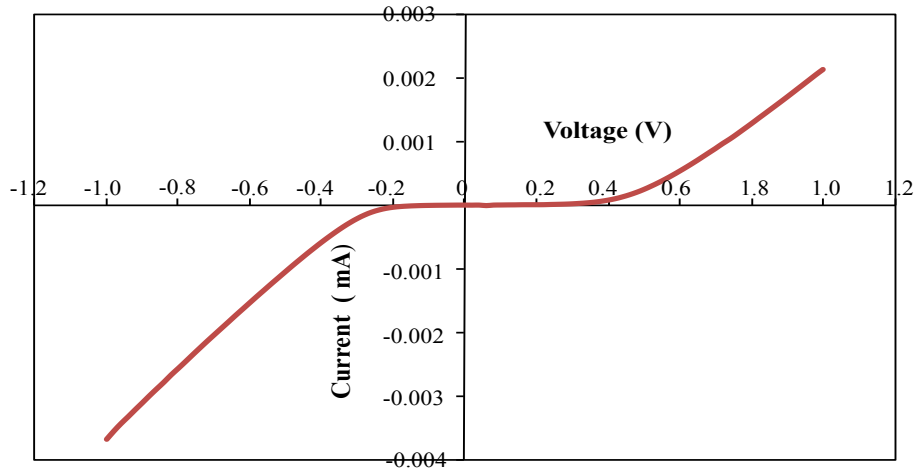


Figure 4: I - V curve in dark for the DSSC utilizing ZnO nanotubes grown at 0.005 M NaOH

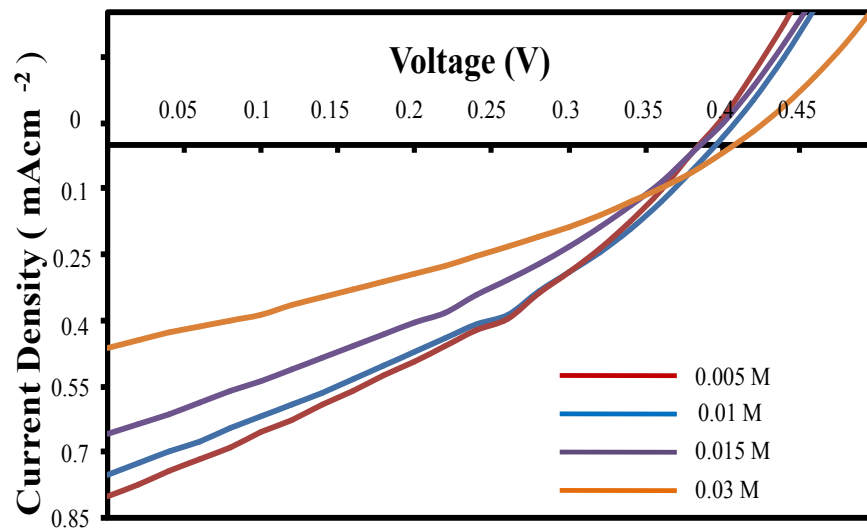


Figure 5: J - V curves under illumination of 100 mW cm^{-2} light for the DSSC utilizing ZnO nanotubes grown at various NaOH concentrations

sensitization effect is due to smaller surface area for dye loading. The working principle of the DSSC is reported by Nazeeruddin et al. [22].

4. Conclusion

The ZnO nanotubes have been synthesized by adding sodium hydroxide (NaOH) in the growth solution containing HMT surfactant and $\text{Zn}(\text{NO}_3)_2$. It was found that the morphology and optical absorption of ZnO nanostructure are significantly affected by the NaOH concentration. The diameter of the nanotubes decreases with the concentration of NaOH. The absorption window increases with the decrease in the NaOH concentration. The photovoltaic parameters decrease as the concentration increases. The DSSC utilizing ZnO nanotubes synthesized at 0.005 M NaOH performs the J_{SC} , V_{OC} , FF and η of 0.80 mA cm^{-2} , 0.38 V , 0.388 and 0.103% , respectively. The highest performance of the cell is due to the widest absorption window of the 0.005 M sample.

Acknowledgement

This work was supported by The Ministry of higher Education of Malaysia under research grant FRGS/2/2013/SG02/UKM/02/8 and GUP-2013-030.

References

1. L. Roza, M.Y.A. Rahman, A.A. Umar, M.M. Salleh, J. Alloys Compd. 618 (2015) 153-158.
2. Z.Z. Zhou, Y. Ding, X.H. Zu, Y.L. Deng, J. Nanopart. Res. 13 (2011)1689-1696.
3. M.Y.A. Rahman, A.A. Umar, R. Taslim, L. Roza, S.K.M. Saad, M.M. Salleh, Int. J. Electroactive Mater. 2 (2014) 4-7.
4. M.S. Akhtar, M.A. Khan, M.S. Jeon, O.-B. Yang, Electrochim. Acta 53 (2008) 7869-7874.
5. G.C. Yi, C.R. Wang, W.I. Park, Semicond. Sci. Tech. 20 (2005) S22-S34.
6. Z.L. Wang, J. Nanosci. Nanotech. 8 (2008) 27-55.

7. S. Rani, P. Suri, P. Shishodia, R.M. Mehra, Solar Energy Mater. Solar Cells 92 (2008) 1639-1645.
8. Q. Zhang, T.P. Chou, B. Russo, S.A. Jenekhe, G. Caou, Electrochem. Commun. 47 (2008) 2402-2406.
9. A.A. Umar, M.Y.A. Rahman, R. Taslim, M.M. Salleh, M. Oyama, Int. J. Electrochem. Sci. 7 (2012) 8384-8393.
10. L. Roza, M.Y.A. Rahman, A.A. Umar, M.M. Salleh, J. Alloys Compd. 618 (2015) 153-158.
11. M.Y.A. Rahman, A.A. Umar, L. Roza, M.M. Salleh, J. Sol. State Electrochem. 16 (2012) 2005-2010.
12. M.Y.A. Rahman, A.A. Umar, L. Roza, M.M. Salleh, J. Sol. State Electrochem. 16 (2012) 3947-3952.
13. B.J. Baxter, E.S. Aydil, Sol. Energy Mater. Sol. Cells 90 (2006) 607-622.
14. A.A. Umar, S. Nafisah, S.K.M. Saad, S.T. Tan, A. Balouch, M.M. Salleh M. Oyama, Sol. Energy Mater. Sol. Cells 122 (2014) 174-182.
15. R. Taslim, M.Y.A. Rahman, M.M. Salleh, A.A. Umar, A. Ahmad, J. Sol. State Electrochem. 14 (2010) 2089-2093.
16. M.Y.A. Rahman, A.A. Umar, L. Roza, M.M. Salleh, Int. J. Electroactive Mater. 1 (2013) 28-35.
17. M.Y.A. Rahman, A.A. Umar, R. Taslim, M.M. Salleh, Electrochim. Acta 88 (2013) 639-643.
18. J.B. Chu, S.M. Huang, D.W. Zhang, Z.Q. Bian, X.D. Li, Z. Sun, X.J. Yin, Appl. Phys A 95 (2009) 849-855.
19. S. Ameen, M.S. Akhtar, H.-K. Seo, Y.S. Kim, H.S. Shin, Chem. Eng. J. 187 (2012) 351-356.
20. M.Y.A. Rahman, A.A. Umar, L. Roza, M.M. Salleh, Russian J. Electrochem. 50 (2014) 1072-1076.
21. M.Y.A. Rahman, A.A. Umar, S.K.M. Saad, M.M. Salleh, A. Ishaq, J. New Mater. Electrochem. Syst. 17 (2014) 33-37.
22. M.K. Nazeeruddin, E. Baranoff, M. Gratzel, Solar Energy 85 (2011) 1172-1178.

© 2015 by the authors. Published by EMS (www.electroactmater.com). This article is an open access article distributed under the terms and conditions of the Creative Commons Attribution license (<http://creativecommons.org/licenses/by/4.0/>)